POLITECNICO DI TORINO
Repository ISTITUZIONALE

Fully biobased UV-cured thiol-ene coatings

Original
Fully biobased UV-cured thiol-ene coatings / Pezzana, L.; Sangermano, M.. - In: PROGRESS IN ORGANIC COATINGS. - ISSN 0300-9440. - ELETTRONICO. - 157:(2021), pp. 106295-(1 of 7). [10.1016/j.porgcoat.2021.106295]

Availability:
This version is available at: 11583/2897094 since: 2021-04-26T14:21:20Z

Publisher:
elsevier

Published
DOI:10.1016/j.porgcoat.2021.106295

Terms of use:

This article is made available under terms and conditions as specified in the corresponding bibliographic description in the repository

Publisher copyright
Elsevier postprint/Author's Accepted Manuscript

© 2021. This manuscript version is made available under the CC-BY-NC-ND 4.0 license
http://creativecommons.org/licenses/by-nc-nd/4.0/.The final authenticated version is available online at:
http://dx.doi.org/10.1016/j.porgcoat.2021.106295

(Article begins on next page)

14 November 2024

FULLY BIOBASED UV-CURED THIOL-ENE COATINGS

L. Pezzana[a], M. Sangermano*,[a]

[a] Politecnico di Torino, Department of Applied Science and Technology, Corso Duca degli Abruzzi 24, 10129 Torino, Italy

ABSTRACT: New fully biobased formulation was developed and UV cured to obtain a polymer network useful for coating applications. Lipoic acid and isosorbide diallyl were used as functional monomer for thiol-ene chemistry. Radical UV curing was used to get the network from the liquid resin. The fully biobased formulation was UV cured and tested. Photorheology was employed to follow the reaction kinetic. Attenuated Total Reflectance-Fourier Transform Infrared Spectroscopy (ATR-FTIR) analysis was done to confirm the cross-linking. Thermal characterization was performed by means of Differential Scanning Calorimetry (DSC). The Tg of the network was comparable with the thiol-ene network previously studied. A complete coating characterization was performed by measuring contact angle, adhesion, and pencil hardness. The obtained results indicated suitable performance for coating applications.

KEY WORD: biobased monomers, thiol-ene, lipoic acid, isosorbide diallyl, coating

1. INTRODUCTION

UV-cCuring of multifunctional monomers is one of the fastest and more efficient methods available to generate three-dimensional polymer networks. Among the advantages of this technology are the high cure speed, the reduced energy consumption and absence of VOC emissions. These advantages have allowed its rapid growth in a large variety of applications, particularly for the fast drying of varnishes, printing inks, and protective coatings [1–3].

Among different UV-induced polymerization mechanism, thiol-ene UV-curable formulations have acquired renewed interest due to the inherent characteristic of this kind of reactions. The formulations are based on a mixture of a multifunctional ene monomers and multifunctional thiols that undergo a step-growth polymerization upon UV irradiation leading to crosslinked networks [4–8].

The ‘‘click’’ thiol-ene chemistry is a very rapid and orthogonal reaction, that proceed almost quantitatively in mild conditions and are not inhibited either by oxygen or humidity. In general, thiol-ene photopolymerization offers many advantages with respect to the traditional acrylate photopolymerization process. Desirable features of thiol-ene photopolymerization includes: fast polymerization rate in air, low shrinkage at high monomer conversion, and most importantly, versatility in the thiol and ene monomers selection [2,9,10].

Recently there is an increase interest in replacing the petroleum-based monomers with bio-resources, both because of an increasing environmental concern as well as because of the prediction of scarcity of petroleum resources. High performance coatings derived from thiol-ene chemistry were already achieved starting from bio-based monomers, such as terpenes [11–13], unsaturated vegetable oils [14,15], and lignin-derivates [16,17]. Lipoic acid and isosorbide represent two available biobased monomers suitable to be functionalized and used in thiol-ene chemistry.

Lipoic acid (LA), discovered in 1953 by Reed [18], is a natural molecule present in human body. It is also present in different plants: potatoes, spinaches, and onions [19]. LA is present in wheat either roots or leaves [20]. The peculiar characteristic is the presence of a disulfide bond in a five-atom ring that can be easily exploited for thiol-ene photopolymerization [21]. LA (Figure 1a) has gained considerable attention as an antioxidant. It exists in two forms, lipoate or dihydrolipoate (reduced

form), that can react with reactive oxygen species such as superoxide radicals, hydroxyl radicals, hypochlorous acid, peroxyl radicals, and singlet oxygen [22]. High molecular weight polymer starting from LA can be synthesized by thermal-activated polymerization [23] and is demonstrate ~~that~~ LA is reactive also to UV irradiation. One of the first study was reported in 1954 [24]; then, Nambu et al. studied the copolymerization with styrene by the ring opening of the five-member cyclic disulfide [25]. Additionally, the five-member cyclic disulfide was copolymerized with vinyl monomers by radical copolymerization [26]. Tang et al. [27] demonstrated the formation of degradable and non-degradable networks. The first contained a significant fraction of backbone disulfide groups formed by radical reaction of LA with ethylacrylate while the second had thioether-type sulfur atoms in the backbones synthetized by thiol-ene chemistry that gave non-degradable properties. Recent studies showed the reactivity of the disulfide to vinyl monomers through UV-curing [28]. The disulfide group, incorporated in the polymer network, reacted with vinyl functionalized dies to obtain a post functionalization of the surface through thiol-ene chemistry [29].

The US Department of Energy introduced isosorbide among the 15 molecules of special interest for biorefinery development (Figure 1b) [30]. The structure of isosorbide was reported in 1946 [31], it is also known as 1,4:3,6-dianhydro-D-glucitol and 1,4:3,6-dianhydro-D-sorbitol [32]. Sugar-based monomers are widely studied as precursor to a variety of new polymers. They are inexpensive, high available and they give high degradability to the final products [33]. Fenouillot et al. [34] and then Gandini et al. [35] have provided ~~a~~ reviews with several possibilities to use isosorbide and its derivates to produce polymers. More recently Aricò et al. [30] presented the great potential of isosorbide to become a suitable platform for biobased monomers for polymerization reactions [36,37], functional materials [38,39], synthesis of pharmaceuticals, surfactants [40], novel organ catalysts [41], and cross-linking agents [42]. Medical device can be made exploiting isosorbide due to the biocompatible features of this sugar-derived polymers [43]. Isosorbide has been used in coating applications. From powder coating [44] to UV curable coating [45,46]. Referring specifically to the thiol-ene chemistry isosorbide was employed by Kristufec et al. [47]. Isosorbide was functionalized by allylation in order to have UV reactive groups. The coating had Tg below room temperature and high cell-viability. The coating showed degradation under biological conditions, but with slower rate when compared to the accelerated basic conditions. Other studies showed the possibility to form an antibacterial and environmentally friendly photocured coating. Silver salt and synthesized phosphonium salt were used in two different studies to provide antibacterial properties. The outcomes suggested the excellent antibacterial properties of the photocured networks [48,49]. All these reported studies had a partial amount of biobased monomer derived from the ene functionality, while the thiol functionality was derived by commercial products as trimethylolpropane tris(3-mercaptopropionate).

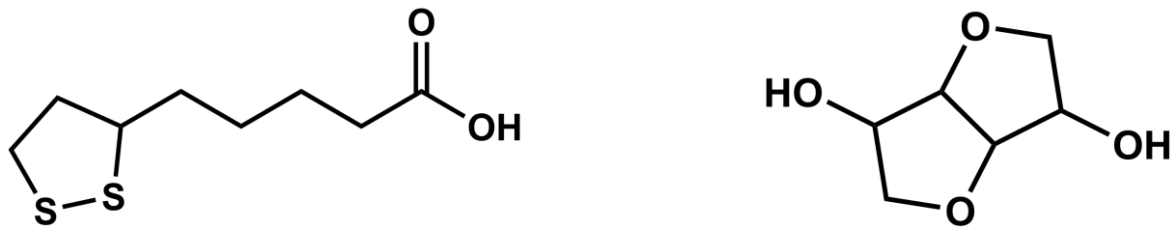

Figure 1. chemical structure of the two biobased monomers used in the study, lipoic acid (left); isosorbide (right).

Within this context, we developed a new fully bio-based thiol-ene photocurable formulation. Lipoic acid was employed as thiol while diallyl isosorbide (IDA) was the ene monomer. The thiol-ene reaction was followed by means of ATR-FTIR and photorheology measurement to evaluate the conversion and the reaction kinetics. Gel content confirmed the formation of a fully crosslinked network. Thermal properties of the coating were studied by DSC analysis. Moreover, coating properties such as contact angle, hardness and adhesion were measured. To have a comparison between the fully biobased formulation and an already used partially biobased formulation, diallyl

isosorbide was also tested with commercially available thiol, trimethylolpropane tris(3-mercaptopropionate) (TRIS).

2. EXPERIMENTAL

2.1. Material

Lipoic acid (LA) and trimethylolpropane tris(3-mercaptopropionate) (TRIS) were purchased by Sigma-Aldrich (Milan, Italy). Chloroform was purchased by Merk KGaA (Milan, Italy). Isosorbide di-allyl (IDA) was supplied by Specific Polymer (Castries, France). The photoinitiator employed was Darocure 1173 provided by BASF (Rome, Italy).

2.2. Photopolymerization

Thio-ene photocurable formulation was prepared by mixing LA and IDA in equimolar ratio with 5 phr of photoinitiator. The formulation containing LA and TRIS had 1 phr of Darocure 1173, Table 1. The photocurable formulations were prepared using the following procedure.

LA (400 mg) was placed in a test tube together with IDA (439 mg). The test tube was stirred for 10 min in an ultrasonic bath at room temperature to allow complete mixing. The photo-initiator, Darocure 1173 (42 mg), was finally added ~~whereafter~~ covering the test tube ~~was covered~~ with aluminum foil and stirred for another 2−3 min to ensure a complete dissolution. A set of films was prepared coating the formulation on a glass slide and irradiating with the UV-lamp for 5 minutes. The thickness of the coatings was 50 μm. The UV irradiation was performed with a Dymax ECE 5000 Flood lamp. The irradiation time was 5 min (150 mW/cm^2). The procedure was repeated for the formulation with TRIS and IDA; the irradiation time was reduced to 2 min and the photoinitiator was added in 1 phr.

Table 1. tested formulation.

Entry	Thiol monomer	(mg)	Ene monomer	(mg)	Photoinitiator	(phr)
1	TRIS	400	IDA	341	Darocure 1173	1
2	LA	400	IDA	439	Darocure 1173	5

2.3. Characterization

2.3.1. Photorheology

Real time p~~P~~hotorheology measurements were performed by means of an Anton Paar MC 302 rheometer (Physica MCR 302, Graz, Styria). The ~~rheometer was set as a plate-plate~~tests were done in a plate-plate geometry equipped with a 25 mm diameter upper disk and a quartz bottom plate~~, the accessory had a diameter of 2.5 cm~~. The distance between the quartz crystal and the plate was 100 μm which corresponds approximately to 150 μL of coating resin. The light source was a Hamamatsu LIGHTINGCURE LC8 equipped with an optic fiber. The intensity of the UV light was 75 mW/cm^2. Oscillatory measurements were performed at constant ~~The conditions for the tests were the following:~~ frequency of 1 Hz, strain of 1 %, in isothermal condition at 25 °C. T~~t~~he lamp was switched on after 60 s in order to stabilize the system before the start of the photopolymerization process.

2.3.2. *Attenuated total Reflectance-Fourier Transform Infrared Spectroscopy (ATR-FTIR)*

Thiol-ene conversion was analyzed by ~~The instrument used for the evaluation of the thiol-ene conversion was a~~ Nicolet iS 50 Spectrometer (Thermo Scientific, Waltham, USA). Spectra ~~Data~~ pre- and post-curing were collected as 32 scans with a spectral resolution of 4.0 cm^{-1}. All data were recorded and handled with the software Omnic from Thermo Fischer Scientific. The photocuring reaction was monitored by the disappearance of the thiol-peak at 2565 cm^{-1} and the reduction of the carbon-carbon double bond peak at 1645 cm^{-1} and the stretching vibration of vinyl caron-hydrogen ~~peak~~ at 925 cm^{-1} for the IDA + TRIS (Entry 1, Table 1). The network formation for the Entry 2 was monitored by the disappearance ~~peak~~ of the C=C peak situated at 1645 cm^{-1} and the C-H peak at 925 cm^{-1}.

2.3.3. *Gel content*

The gel content percentage (% gel) of the cured films was determined by measuring the weight loss after 24 h extraction with chloroform. The samples after the immersion were allowed to dry for 24 h in air. % gel was calculated according to Equation (1):

$$\%gel = \frac{W_1}{W_0} \times 100 \quad (1)$$

where W_1 is the weight of the dry film after the treatment with chloroform and W_0 is the weight of the dry sample before the treatment.

2.3.4. *Differential scanning calorimeter (DSC)*

The DSC analysis was performed on a Mettler Toledo DSC-1 equipped with Gas Controller GC100 (Columbus, Massachusetts, USA). The test method was made by two heating scans: ~~The method used was the follow: the starting temperature was set as 25 °C;~~ the first heating wentgoes from 25 to 100 °C; then the temperature was ~~maintained~~ held at 100 °C for 2 min in order to stabilize the sample, after that the chamber was ~~again~~ cooled until -70 °C was reached and then this temperature was kept ~~maintained~~ for 2 min, finally was applied a second heating from -70 °C to 100 °C. The heating and the cooling rates were set at 10 °C/min and the analysis was performed in a nitrogen atmosphere with a flow rate 20 mL/min. The Tg values were calculated from the second heating curves. In this study 40 µL aluminum pans were used. The data were analyzed with Mettler Toledo STARe software V9.2.

2.3.5. *Coating properties*

The pencil hardness and the adhesion were measured according to the standard ASTM D3363 [50] and ASTM D3359 [51]. Pencils of different grades (~~For the hardness different pencil were used~~ from 8 B to 8 H) were used to perform the hardness test. The hardness of the coating was taken as that of the pencil that produced a cut on the surface of the film. Eclometer 107, as cross hatch cutter, was used for determining the adhesion. The insert number 2 was used as cutter. The adhesion percentage was evaluated as the number of squared remained attached on the substrates. The films were photocured on glass substrate. ~~The c~~Contact angle measurements ~~were~~was performed by Drop Shape Analyzer, DSA100, Krüss (Germany), equipped with a video camera. The reported results are an average of at least 5 water droplets.

3. RESULT AND DISCUSSION

The photocuring process of the thiol-ene formulations was investigated by means of photorheology; in Figure 2 the storage modulus as a function of irradiation time is reported for the fully bio-based formulation (LA and IDA in equimolar ratio) and compare with the formulation containing TRIS as thiol-monomer.

When comparing the two formulations it can be observed that the reaction between TRIS and IDA started immediately after the lamp turned on while the LA and IDA reaction is much slower. The storage modulus of IDA + LA had an induction time of 180 s then the reaction started.

This can be explained taking into consideration the different nature of the thiol monomer used. The commercial one, TRIS, had already –S–H bonds available for the reaction. Instead, the biobased LA had a disulfide group that needs to break upon irradiation to generate the reactive specie (–S•) necessary for the click thiol-ene reaction. Previous studies demonstrated the reactivity of disulfide group towards UV irradiation [27,52] corroborating the reactivity of this group in this thiol-ene reaction. By irradiation of the disulfide group, the radical is formed thanks the energy given through the UV irradiation; thus, the delay time of the reaction of IDA-LA formulation is due to the production of the reactive specie that can start the reaction.

Once the reaction started, the slope of the curve increased reaching the plateau in about 5 minutes. A higher amount of photoinitiator was necessary to promote the UV-induced crosslinking reaction of the fully biobased formulation (5 phr) with respect with the IDA + TRIS (1 phr). A scheme of the fully biobased formed network is illustrated in Scheme 1.

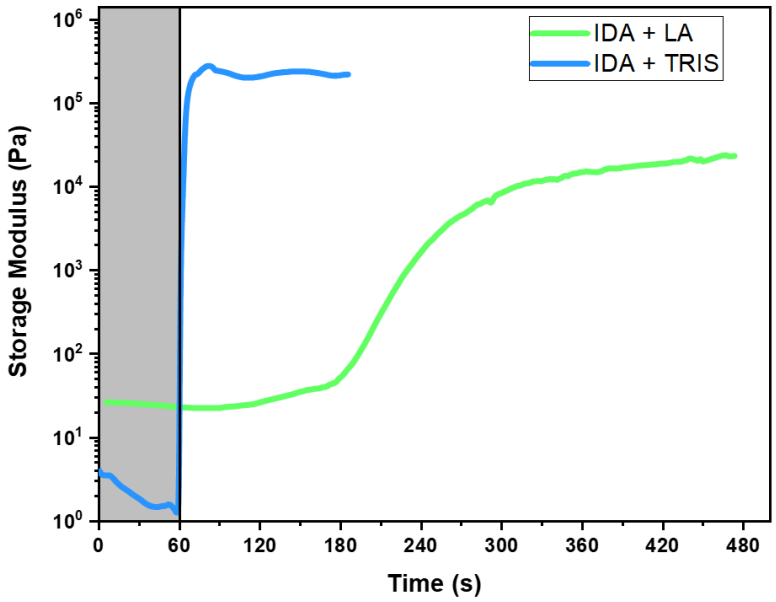

Figure 2. Photorheology results, after 60 s the UV lamp was turned on. Trend of the storage modulus for the fully biobased formulation (green curve) and partial biobased resin (blu curve).

To confirm the curing process, ATR-FTIR analyses were done comparing the spectra before and after irradiation. The ATR-FTIR spectra are collected in Figure 3 for the fully bio-based formulation and for the IDA-TRIS formulation.

Regarding the IDA-TRIS formulation, different peaks can be followed to validate the photo crosslinking reaction [47–49]: stretching vibration of thiol peak (S–H) at 2565 cm^{-1}, stretching vibration of ene peak (C=C) at 1645 cm-1, and C–H vibration of vinyl group at 925 cm^{-1} were monitored, (zoom of the spectra are reported in Figure 4). Both thiol and ene peaks showed a complete disappearance after 2 min of irradiation, indicating the fully conversion upon irradiation. This confirms the stochiometric reaction, typical of the thiol-ene step-growth mechanism.

Instead, the network formation for the formulation IDA + LA was followed by the ene peaks at 1645 cm^{-1} (C=C), and 925 cm^{-1} (C–H). The Figure 3 shows the spectra before and after irradiation with an enlargement in Figure 4. The thiol bond peak cannot be considered since the structure of the reagent (LA) had disulfide groups and no free thiols. However, considering the typical step-growth mechanism for thiol-ene reaction, it is enough to follow the disappearance of the ene peaks to evaluate the thiol-ene conversion.

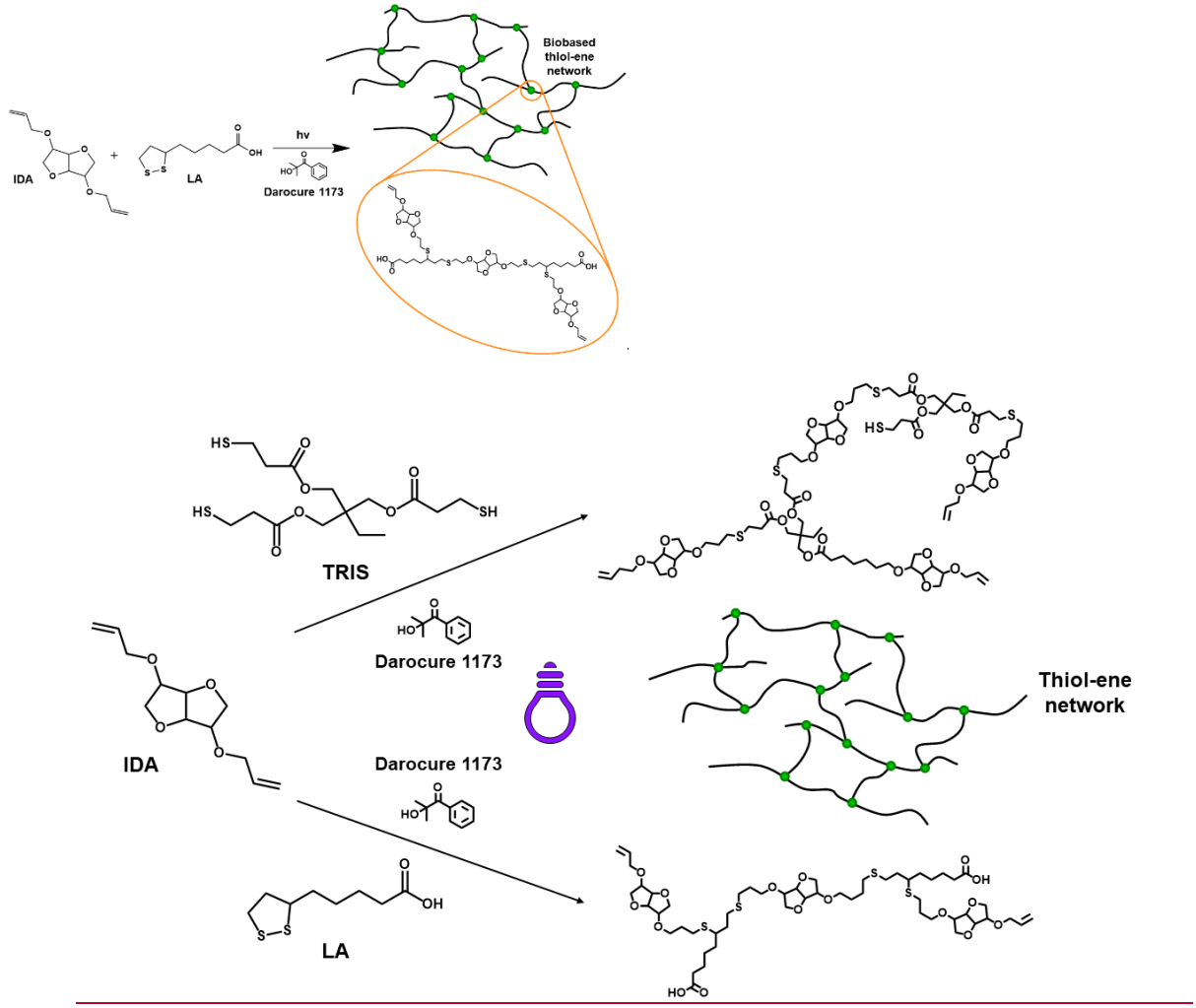

Scheme 1. A schematic illustration showing the thiol-ene photopolymerization of IDA and LA in the presence of Darocure 1173, (Entry 2, Table 1).

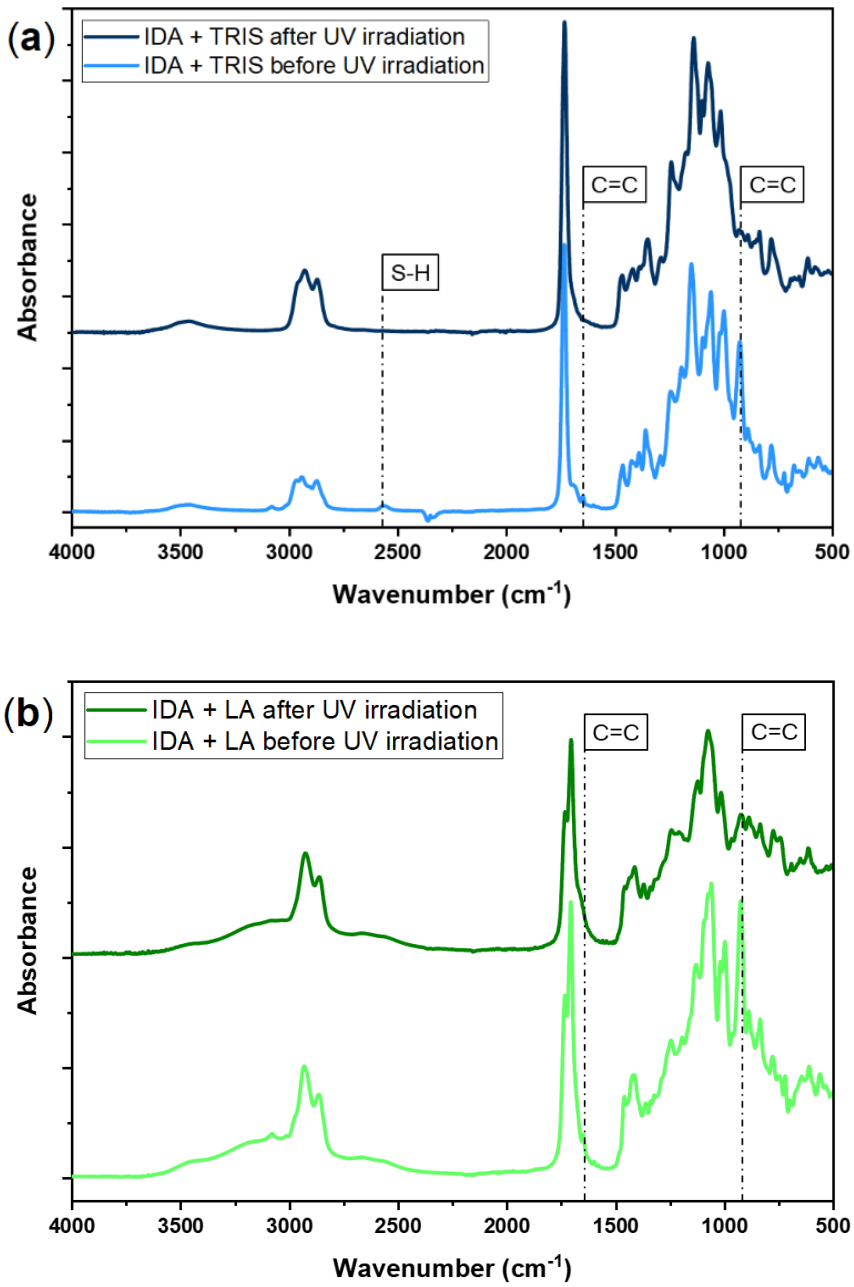

Figure 3. ATR-FTIR spectra for the tested resins: (**a**) spectra before- (light blue) and after irradiation (blue) for the partially biobased resin; (**b**) spectra before- (light green) and after irradiation (dark green) for the fully biobased resin.

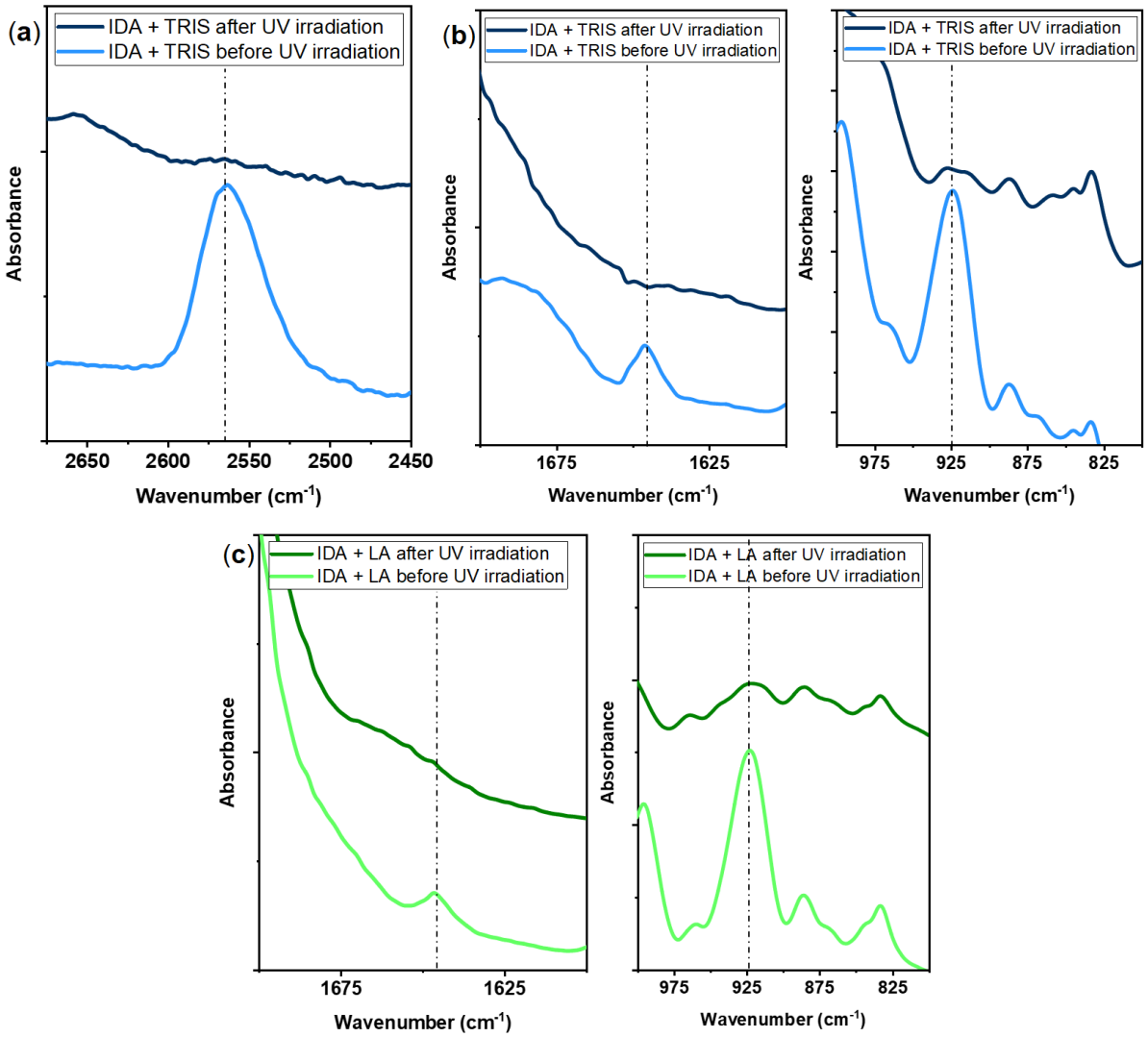

Figure 4. Zoom of the characteristic peaks taken into account to confirm the curing: (**a**) partial biobased formulation; thiol peak at 2565 cm^{-1}; (**b**) partial biobased formulation; ene peaks centered at 1645 cm^{-1}, and 925 cm^{-1}; (**c**) fully biobased resin, C=C peak centered at 1645 cm^{-1}, and C–H peak at 925 cm^{-1}.

Tack-free films were achieved after irradiation and gel content was determined after 24 h of immersion in chloroform. The fully biobased formulation reached 88 % of gel content, while the partially biobased 95 %, (data collected in Table 2). Despite the slower kinetic the fully biobased formulation reached high value of gel content demonstrating the achievement of a fully crosslinked network. The gel content of the partial biobased formulation was in accordance with the previous study [49]. The lower gel content percentage of the fully biobased formulation could be explained take into account the slower kinetics with respect to the use of the tri-thiol monomer and therefore, the possibility that some disulfide group did not react properly. This is confirmed by the uncomplete disappearance of the ene peaks after irradiation.

Thermal analysis was performed on crosslinked network by DSC. The Tg of the two crosslinked materials were comparable, the fully biobased coating had a Tg of −14 °C while the partially biobased –12 °C. These results were comparable with the previous reported in literature [48]. The new fully biobased resin showed similar thermal behavior to the formulation containing the commercial thiol. Thus, LA can be considered as a bio-derived alternative to the commercially available thiol, achieving similar properties for the crosslinked coating.

The thermal decomposition behavior of the two different crosslinked films was evaluated by TGA. The curves are reported in Figure 6. The fully biobased coating degraded at lower temperature with respect IDA + TRIS one. The temperature of maximum weight loss degradation was around 320 °C for IDA + LA, instead for the partially biobased was at 370 °C demonstrating higher thermal stability. The onset temperature, T_5, evaluated as the start of the degradation (5% wight loss temperature) were in accordance with the Tmax. In fact, the fully biobased had lower T_5 than partially biobased formulation. IDA + LA had T_5 of 235 °C while T_5 for IDA + TRIS was around 345°C. The difference of the degradation could be explained considering the different chemical structure of the two employed thiols: bifunctional biobased lipoic acid and trifunctional commercial trimethylolpropane tris(3-mercaptopropionate). [49].

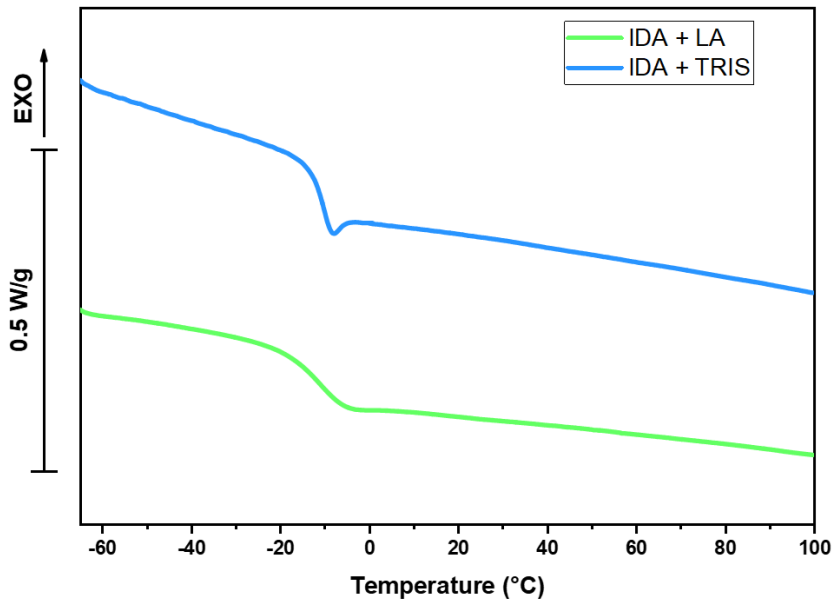

Figure 5: DSC curves; fully biobased formulation (green curve) and partial biobased resin (blu curve).

Table 2: result of the analyses performed on the coatings.

FORMULATION	Tg[1] (°C)	% gel	Contact angle (°)	Pencil Hardness	Adhesion (%)
IDA + TRIS	− 12 ± 1	95 ± 2	85 ± 2	8 H	84%
IDA + LA	− 14 ± 1	88 ± 1	88 ± 3	5 H	92 %

[1] Tg evaluated as mid-point of the curves by means of DSC analysis.

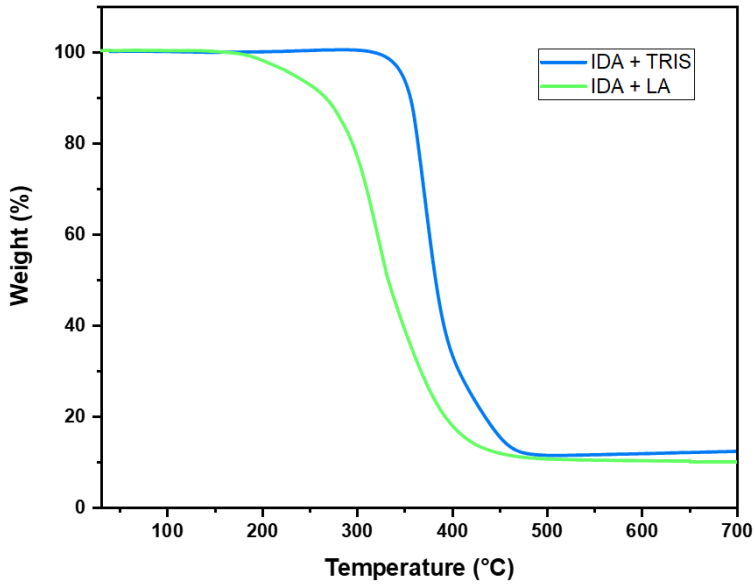

Figure 6: TGA curves; fully biobased formulation (green curve) and partial biobased resin (blu curve).

The coating properties of the fully biobased formulation were comparable and some even better with respect to the partial biobased IDA-TRIS. The adhesion on glass substrate reached 92 % for IDA + LA while IDA + TRIS achieved 85 %. The acidic nature of the lipoic acid can influence the adhesion on the glass substrate making stronger interaction with the surface. The pencil hardness of the two coatings reached 5 H for the fully biobased and 8 H for the partially biobased. The contact angle with water was comparable for both compositions attesting around 85 ° for IDA + TRIS and 88° for IDA + LA.

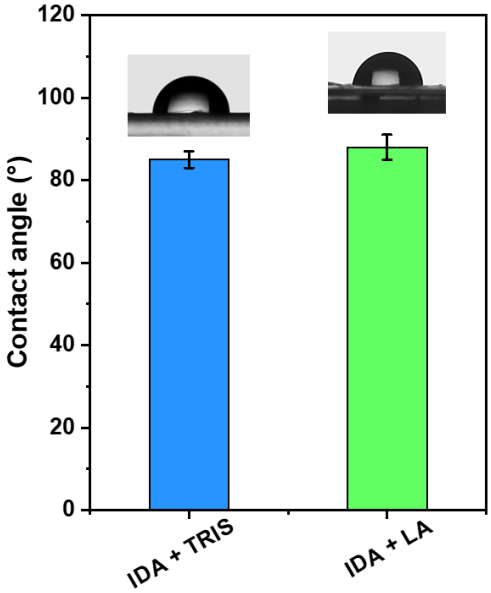

~~**Figure 6:** Contact angle result for the IDA+ TRIS biobased (blue) and the IDA + LA fully biobased resin (green) UV-cured coatings.~~

4. CONCLUSION

In this work it was demonstrated the possibility to achieve a new fully biobased network exploiting the ~~the~~ lipoic acid ~~isosorbide~~ and isosorbide diallyl ~~acid as~~ thiol-ene monomers. The network was created by exposing to UV light the formulation involving the thiol-ene click chemistry. The photorheology measurement allowed to investigate the kinetic of network formation. The ATR-FTIR analysis, confirmed the photo curing by the disappearance of the allylic double bond peaks. The Tg of the fully UV-biobased UV-cured coating was comparable with the Tg for the partially bio-based crosslinked formulation containing TRIS and IDA as thiol-ene monomer. These results showed a possible approach to substitute the thiol monomer with a bio-based one achieving the possibility to obtain a fully bio-based thiol-ene UV-curable formulation. The coating properties, such as adhesion, hardness and contact angle, were in the trend with the TRIS + IDA UV-cured formulation. In conclusion, we report a new green alternative to develop a resin designed for coating applications.

Declaration of Competing Interest

The authors declare that they have no known competing financial interests or personal relationships that could have appeared to influence the work reported in this paper.

REFERENCES

[1] A.B. Scranton, C.N. Bowman, R.W. Peiffer, Photopolymerization: fundamentals and applications, ACS Publications, 1997.

[2] N.B. Cramer, C.N. Bowman, Kinetics of thiol-ene and thiol-acrylate photopolymerizations with real-time Fourier transform infrared, J. Polym. Sci. Part A Polym. Chem. 39 (2001) 3311–3319. https://doi.org/10.1002/pola.1314.

[3] M. Sangermano, Advances in cationic photopolymerization, Pure Appl. Chem. 84 (2012) 2089–2101. https://doi.org/https://doi.org/10.1351/PAC-CON-12-04-11.

[4] S.C. Ligon, B. Husár, H. Wutzel, R. Holman, R. Liska, Strategies to reduce oxygen inhibition in photoinduced polymerization, Chem. Rev. 114 (2014) 577–589. https://doi.org/10.1021/cr3005197.

[5] M. Sangermano, N. Razza, J.V. Crivello, Cationic UV-curing: Technology and applications, Macromol. Mater. Eng. 299 (2014) 775–793. https://doi.org/10.1002/mame.201300349.

[6] M. Sangermano, Recent advances in cationic photopolymerization, J. Photopolym. Sci. Technol. 32 (2019) 233–236. https://doi.org/10.2494/photopolymer.32.233.

[7] Y. Yagci, Photoinitiated cationic polymerization of unconventional monomers, Macromol. Symp. 240 (2006) 93–101. https://doi.org/10.1002/masy.200650812.

[8] C. Noè, M. Hakkarainen, M. Sangermano, Cationic uv-curing of epoxidized biobased resins, Polymers (Basel). 13 (2021) 1–16. https://doi.org/10.3390/polym13010089.

[9] C.E. Hoyle, C.N. Bowman, Thiol-ene click chemistry, Angew. Chemie - Int. Ed. 49 (2010) 1540–1573. https://doi.org/10.1002/anie.200903924.

[10] S.K. Reddy, O. Okay, C.N. Bowman, Network development in mixed step-chain growth thiol-vinyl photopolymerizations, Macromolecules. 39 (2006) 8832–8843. https://doi.org/10.1021/ma060249m.

[11] M. Claudino, J.M. Mathevet, M. Jonsson, M. Johansson, Bringing d-limonene to the scene of bio-based thermoset coatings via free-radical thiol-ene chemistry: Macromonomer synthesis, UV-curing and thermo-mechanical characterization, Polym. Chem. 5 (2014) 3245–3260. https://doi.org/10.1039/c3py01302b.

[12] M. Claudino, I. Van Der Meulen, S. Trey, M. Jonsson, A. Heise, M. Johansson, Photoinduced thiol-ene crosslinking of globalideε-caprolactone copolymers: Curing performance and resulting thermoset properties, J. Polym. Sci. Part A Polym. Chem. 50 (2012) 16–24. https://doi.org/10.1002/pola.24940.

[13] A. Stamm, M. Tengdelius, B. Schmidt, J. Engström, P.O. Syrén, L. Fogelström, E. Malmström, Chemo-enzymatic pathways toward pinene-based renewable materials, Green Chem. 21 (2019) 2720–2731. https://doi.org/10.1039/C9GC00718K.

[14] O. Türünç, M. Firdaus, G. Klein, M.A.R. Meier, Fatty acid derived renewable polyamides via thiol-ene additions, Green Chem. 14 (2012) 2577–2583. https://doi.org/10.1039/c2gc35982k.

[15] M. Claudino, M. Johansson, M. Jonsson, Thiol-ene coupling of 1,2-disubstituted alkene monomers: The kinetic effect of cis/trans-isomer structures, Eur. Polym. J. 46 (2010) 2321–2332. https://doi.org/10.1016/j.eurpolymj.2010.10.001.

[16] M. Fache, E. Darroman, V. Besse, R. Auvergne, S. Caillol, B. Boutevin, Vanillin, a promising biobased building-block for monomer synthesis, Green Chem. 16 (2014) 1987–1998. https://doi.org/10.1039/c3gc42613k.

[17] L. Pezzana, M. Mousa, E. Malmström, M. Johansson, M. Sangermano, Bio-based monomers for UV-curable coatings: allylation of ferulic acid and investigation of photocured thiol-ene network, Prog. Org. Coatings. 150 (2021) 105986. https://doi.org/https://doi.org/10.1016/j.porgcoat.2020.105986.

[18] L.J. Reed, Metabolic Functions of Thiamine and Lipoic Acid, Physiol. Rev. 33 (1953) 544–559. https://doi.org/10.1152/physrev.1953.33.4.544.

[19] F. Navari-Izzo, M.F. Quartacci, C. Sgherri, Lipoic acid: a unique antioxidant in the detoxification of activated oxygen species, Plant Physiol. Biochem. 40 (2002) 463–470. https://doi.org/https://doi.org/10.1016/S0981-9428(02)01407-9.

[20] C. Sgherri, M.F. Quartacci, R. Izzo, F. Navari-Izzo, Relation between lipoic acid and cell redox status in wheat grown in excess copper, Plant Physiol. Biochem. 40 (2002) 591–597. https://doi.org/https://doi.org/10.1016/S0981-9428(02)01421-3.

[21] T. Chen, M. Qiu, J. Zhang, H. Sun, C. Deng, Z. Zhong, Integrated Multifunctional Micelles Co-Self-Assembled from Polypeptides Conjugated with Natural Ferulic Acid and Lipoic Acid for Doxorubicin Delivery, ChemPhysChem. 19 (2018) 2070–2077. https://doi.org/10.1002/cphc.201701367.

[22] L. Packer, E.H. Witt, H.J. Tritschler, Alpha-lipoic acid as a biological antioxidant, Free Radic. Biol. Med. 19 (1995) 227–250. https://doi.org/10.1016/0891-5849(95)00017-R.

[23] A. Kisanuki, Y. Kimpara, Y. Oikado, N. Kado, M. Matsumoto, K. Endo, Ring-opening polymerization of lipoic acid and characterization of the polymer, J. Polym. Sci. Part A Polym. Chem. 48 (2010) 5247–5253. https://doi.org/https://doi.org/10.1002/pola.24325.

[24] J.A. Barltrop, P.M. Hayes, M. Calvin, The Chemistry of 1,2-Dithiolane (Trimethylene Disulfide) as a Model for the Primary Quantum Conversion Act in Photosynthesis1a, J. Am. Chem. Soc. 76 (1954) 4348–4367. https://doi.org/10.1021/ja01646a029.

[25] Y. Nambu, M.H. Acar, T. Suzuki, T. Endo, Thermal and photoinitiated copolymerization of the cyclic disulfide lipoamide with styrene, Die Makromol. Chemie. 189 (1988) 495–500. https://doi.org/https://doi.org/10.1002/macp.1988.021890302.

[26] T. Suzuki, N. Yoko, E. Takeshi, Radical Copolymerization of Lipoamide with Vinyl Monomers, Macromolecules. 23 (1990) 1579–1582. https://doi.org/10.1021/ma00208a004.

[27] H. Tang, N. V. Tsarevsky, Lipoates as building blocks of sulfur-containing branched macromolecules, Polym. Chem. 6 (2015) 6936–6945. https://doi.org/10.1039/c5py01005e.

[28] M. Finnveden, S. Brännström, M. Johansson, E. Malmström, M. Martinelle, Novel sustainable synthesis of vinyl ether ester building blocks, directly from carboxylic acids and the corresponding hydroxyl vinyl ether, and their photopolymerization, RSC Adv. 8 (2018) 24716–24723. https://doi.org/10.1039/c8ra04636k.

[29] S. Brännström, M. Johansson, E. Malmström, Enzymatically Synthesized Vinyl Ether-Disulfide Monomer Enabling an Orthogonal Combination of Free Radical and Cationic Chemistry toward Sustainable Functional Networks, Biomacromolecules. 20 (2019) 1308–1316. https://doi.org/10.1021/acs.biomac.8b01710.

[30] F. Aricò, Isosorbide as biobased platform chemical: Recent advances, Curr. Opin. Green Sustain. Chem. 21 (2020) 82–88. https://doi.org/10.1016/j.cogsc.2020.02.002.

[31] R.C. Hockett, H.G. Fletcher, E.L. Sheffield, R.M. Goepp, S. Soltzberg, Hexitol Anhydrides. The Structure of Isosorbide, a Crystalline Dianhydrosorbitol, J. Am. Chem. Soc. 68 (1946) 927–930. https://doi.org/10.1021/ja01210a003.

[32] M. Rose, R. Palkovits, Isosorbide as a renewable platform chemical for versatile applications-quo vadis?, ChemSusChem. 5 (2012) 167–176. https://doi.org/10.1002/cssc.201100580.

[33] J.A. Galbis, M.G. García-Martín, Chapter 5 - Sugars as Monomers, in: M.N. Belgacem, A.B.T.-M. Gandini Polymers and Composites from Renewable Resources (Eds.), Elsevier, Amsterdam, 2008: pp. 89–114. https://doi.org/https://doi.org/10.1016/B978-0-08-045316-3.00005-3.

[34] F. Fenouillot, A. Rousseau, G. Colomines, R. Saint-Loup, J.P. Pascault, Polymers from renewable 1,4:3,6-dianhydrohexitols (isosorbide, isomannide and isoidide): A review, Prog. Polym. Sci. 35 (2010) 578–622. https://doi.org/10.1016/j.progpolymsci.2009.10.001.

[35] A. Gandini, T.M. Lacerda, From monomers to polymers from renewable resources: Recent advances, Prog. Polym. Sci. 48 (2015) 1–39. https://doi.org/10.1016/j.progpolymsci.2014.11.002.

[36] D.J. Saxon, M. Nasiri, M. Mandal, S. Maduskar, P.J. Dauenhauer, C.J. Cramer, A.M. Lapointe, T.M. Reineke, Architectural Control of Isosorbide-Based Polyethers via Ring-Opening Polymerization, J. Am. Chem. Soc. 141 (2019) 5107–5111. https://doi.org/10.1021/jacs.9b00083.

[37] Z. Mi, Z. Liu, C. Tian, X. Zhao, H. Zhou, D. Wang, C. Chen, Soluble polyimides containing 1,4:3,6-dianhydro-d-glucidol and fluorinated units: Preparation, characterization, optical, and dielectric properties, J. Polym. Sci. Part A Polym. Chem. 55 (2017) 3253–3265. https://doi.org/10.1002/pola.28700.

[38] X. Feng, A.J. East, W.B. Hammond, Y. Zhang, M. Jaffe, Overview of advances in sugar-based polymers, Polym. Adv. Technol. 22 (2011) 139–150. https://doi.org/10.1002/pat.1859.

[39] C. Li, J. Dai, X. Liu, Y. Jiang, S. Ma, J. Zhu, Green Synthesis of a Bio-Based Epoxy Curing Agent from Isosorbide in Aqueous Condition and Shape Memory Properties Investigation of the Cured Resin, Macromol. Chem. Phys. 217 (2016) 1439–1447. https://doi.org/10.1002/macp.201600055.

[40] J.-E. Cho, D.-S. Sim, Y.-W. Kim, J. Lim, N.-H. Jeong, H.-C. Kang, Selective Syntheses and Properties of Anionic Surfactants Derived from Isosorbide, J. Surfactants Deterg. 21 (2018) 817–826. https://doi.org/https://doi.org/10.1002/jsde.12182.

[41] M. Janvier, S. Moebs-Sanchez, F. Popowycz, Bio-Based Amides from Renewable Isosorbide by a Direct and Atom-Economic Boric Acid Amidation Methodology, European J. Org. Chem. 2016 (2016) 2308–2318. https://doi.org/10.1002/ejoc.201600186.

[42] S. Ma, D.C. Webster, F. Jabeen, Hard and Flexible, Degradable Thermosets from Renewable Bioresources with the Assistance of Water and Ethanol, Macromolecules. 49 (2016) 3780–3788. https://doi.org/10.1021/acs.macromol.6b00594.

[43] J. Lammel-Lindemann, I.A. Dourado, J. Shanklin, C.A. Rodriguez, L.H. Catalani, D. Dean, Photocrosslinking-based 3D printing of unsaturated polyesters from isosorbide: A new material for resorbable medical devices, Bioprinting. 18 (2020) e00062. https://doi.org/10.1016/j.bprint.2019.e00062.

[44] B.A.J. Noordover, A. Heise, P. Malanowksi, D. Senatore, M. Mak, L. Molhoek, R. Duchateau, C.E. Koning, R.A.T.M. van Benthem, Biobased step-growth polymers in powder coating applications, Prog. Org. Coatings. 65 (2009) 187–196. https://doi.org/10.1016/j.porgcoat.2008.11.001.

[45] G. Wei, H. Xu, L. Chen, Z. Li, R. Liu, Isosorbide-based high performance UV-curable reactive diluents, Prog. Org. Coatings. 126 (2019) 162–167. https://doi.org/10.1016/j.porgcoat.2018.10.028.

[46] A.A. Gadgeel, S.T. Mhaske, Synthesis and characterization of UV curable polyurethane acrylate derived from α-Ketoglutaric acid and isosorbide, Prog. Org. Coatings. 150 (2021) 105983. https://doi.org/10.1016/j.porgcoat.2020.105983.

[47] T.S. Kristufek, S.L. Kristufek, L.A. Link, A.C. Weems, S. Khan, S.M. Lim, A.T. Lonnecker, J.E. Raymond, D.J. Maitland, K.L. Wooley, Rapidly-cured isosorbide-based cross-linked polycarbonate elastomers, Polym. Chem. 7 (2016) 2639–2644. https://doi.org/10.1039/c5py01659b.

[48] C. Lorenzini, A. Haider, I.K. Kang, M. Sangermano, S. Abbad-Andalloussi, P.E. Mazeran, J. Lalevée, E. Renard, V. Langlois, D.L. Versace, Photoinduced Development of Antibacterial Materials Derived from Isosorbide Moiety, Biomacromolecules. 16 (2015) 683–694. https://doi.org/10.1021/bm501755r.

[49] E. Çakmakçi, F. Şen, M.V. Kahraman, Isosorbide Diallyl Based Antibacterial Thiol-Ene Photocured Coatings Containing Polymerizable Fluorous Quaternary Phosphonium Salt, ACS Sustain. Chem. Eng. 7 (2019) 10605–10615. https://doi.org/10.1021/acssuschemeng.9b01161.

[50] ASTM D3363-05, Standard Test Method for Film Hardness by Pencil Test, ASTM Int. (2005). https://doi.org/10.1520/D3363-05.

[51] ASTM D3359-17, Standard Test Methods for Rating Adhesion by Tape Test, ASTM Int. (2017). https://doi.org/10.1520/D3359-17.

[52] D. Mishra, S. Wang, S. Michel, G. Palui, N. Zhan, W. Perng, Z. Jin, H. Mattoussi, Photochemical transformation of lipoic acid-based ligands: Probing the effects of solvent, ligand structure, oxygen and pH, Phys. Chem. Chem. Phys. 20 (2018) 3895–3902. https://doi.org/10.1039/c7cp06350d.